Chinese Chemical Letters 32 (2021) 3322–3330

Contents lists available at ScienceDirect

Chinese Chemical Letters

journal homepage: www.elsevier.com/locate/cclet

Review

Rim-differentiated pillar[5]arenes

Lintao Wu[a], Chun Han[a], Xiaobi Jing[c], Yong Yao[b,*]

[a] Department of Chemistry, Changzhi University, Changzhi 046011, China
[b] School of Chemistry and Chemical Engineering, Nantong University, Nantong 226019, China
[c] School of Chemistry and Chemical Engineering, Yangzhou University, Yangzhou 225009, China

ARTICLE INFO

Article history:
Received 25 February 2021
Revised 20 April 2021
Accepted 22 April 2021
Available online 28 April 2021

Keywords:
Pillar[5]arene
Rim-differentiated
Self-assembly
Biological application
Controlled release

ABSTRACT

Pillar[5]arenes, designed and prepared by Ogoshi *et al.* in 2008 initially, refer to fifth classical macrocyclics. Among a wide range of pillar[5]arenes, rim-differentiated pillar[5]arenes containing five identical substituents on one rim and five different identical groups on the other rims are considered the most noteworthy type of pillar[5]arenes. As compared with the perfunctionalized pillar[5]arene, the self-assembly properties of rim-differentiated pillar[5]arenes have more varieties. On the other hand, in comparison with other types of pillar[5]arenes, the rim-differentiated pillar[5]arenes exhibit a more rigid symmetrical structure. In the present review, the synthetic methods, host-guest interactions, self-assembly properties and applications of rim-differentiated pillar[5]arenes are summarized. Hopefully, this review will be conducive to researchers in macrocyclic supramolecular chemistry.

© 2021 Published by Elsevier B.V. on behalf of Chinese Chemical Society and Institute of Materia Medica, Chinese Academy of Medical Sciences.

1. Introduction

Over the past decades, macrocyclic hosts (*e.g.*, cyclodextrins [1], cucurbiturils [2], and calixarenes [3]) have aroused considerable attention for their amazing conformational and physicochemical host-guest properties. Pillar[*n*]arenes, initially discovered in 2008, were refer to the fifth classical macrocycles [4]. The repeating unites of pillar[*n*]arene are connected by the methylene bridge at the *para*-position, which forms a unique symmetrical pillar-like architecture, inconsistent with basket-shaped structure $-CH_2-$ bridged calixarenes [4]. Pillar[*n*]arenes, for their symmetrical pillar-like structure, can act as a platform for chemical modification, as well as associate with tremendous guest molecules via host-guest interactions [4b–4h]. All the mentioned advantages can be exploited to synthesize tailored pillar[*n*]arenes with targeted applications, which makes them the acutal versatile hosts [5].

Given the substitution units of the pillar[5]arene that are attributed to functionalization, pillar[5]arenes can fall to six categories (Fig. 1) [5a]. The first is monofunctionalized pillar[5]arene, the substitution at one reactive position on a cavitand allows for the addition of novel features without altering its ability to recognize guests significantly [5b,c]. The second one refers to difunctionalized pillar[5]arene, of which two reactive positions are substituted. It consists of five constitutional isomers, each exhibiting more or less different properties [5d–g]. The third represents perfunctionalized pillar[5]arene with ten identical substituents in ten reactive positions. This is the most convenient way to change the properties of pillar[*n*]arene, since this pillar[5]arene is easy to synthesize and achieves a high yield [5h,i]. The fourth one is termed as phenylene-substituted pillar[5]arene, in which functionalization is extended to the hydroquinone position, which are or-

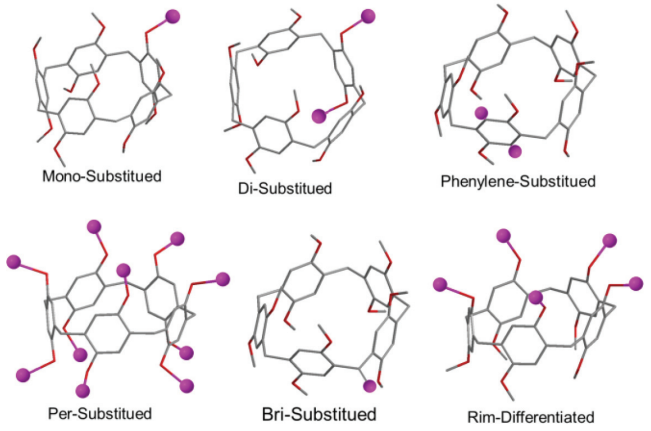

Fig. 1. Six types of functionalized pillar[5]arene, wherein generic functional groups are represented by pink spheres.

* Corresponding author.
E-mail address: yaoyong1986@ntu.edu.cn (Y. Yao).

https://doi.org/10.1016/j.cclet.2021.04.046
1001-8417/© 2021 Published by Elsevier B.V. on behalf of Chinese Chemical Society and Institute of Materia Medica, Chinese Academy of Medical Sciences.

tho to both the methylene bridges and oxygen substituents [5j–l]. This pillar[5]arene can expand the structural diversity. The fifth one is bridge-substituted pillar[5]arene, whose substitution site is the $-CH_2-$ between the aromatic rings [5m]. The last type, termed as rim-differentiated pillar[5]arene (RDP[5]), covers five identical substituents on one rim and five identical substituents on another rim.

As compared with the perfunctionalized pillar[5]arene, the self-assembled properties of RDP[5]s are more diversified. Besides, as compared with other types of pillar[5]arene, the RDP[5]s exhibit a more rigid symmetrical structure to achieve host-guest interactions [6a]. However, the largest challenge facing RDP[5]s is that the synthesis yield is insufficiently high for large-scale applications. Accordingly, a general method should be urgently developed to synthesize RDP[5]s with high yield. Although many reviews about pillar[*n*]arenes have been reported, there was no review about rim-differentiated pillar[5]arene [6b–f]. In this review, the synthetic methods, host-guest interactions, self-assembly properties and applications of RDP[5]s are systematically summarized. Hopefully, this review will be conducive to researchers in macrocyclics-based supramolecular chemistry.

2. Synthetic methods of rim-differentiated pillar[5]arenes

The first RDP[5] **3** was synthesized in 2010 with one-step cyclization method. The defect of this method is that the separation of **3** from its isomers is difficult, and the yield is significantly low, greatly limiting the large-scale application of RDP[5]s [7]. It was not until 2018 that Sue *et al.* facilitated the synthesis of RDP[5]s and proposed the "pre-oriented" synthetic strategy. Though this method can improve the yield of RDP[5]s, the synthesis of the monomer that fabricates RDP[5]s is difficult, so there are limited types of RDP[5]s that can be synthesized [9]. In 2019, they proposed a novel method termed as functionalization at will on the basis of "pre-oriented". Subsequently, the synthesis of RDP[5]s has accessed into a new level [10].

2.1. One-step cyclization

The one-step cyclization strategy refers to the reaction of asymmetrically substituted 1,4-dialkoxybenzene monomers with paraformaldehyde catalyzed by Lewis acid in the solvent (*e.g.*, 1,2-dichloroethane, dichloromethane or chloroform), at room temperature, and the application of silica gel column chromatography to separate the desired RDP[5]s [7]. Moreover, such a method is known as the statistical process. With this method, considerable RDP[5]s were synthesized in the initial stage (Fig. 2a) [7,8,15–26]. For instance, the famous RDP[5] **7**, containing five amino groups as the hydrophilic head and five alkyl chain as the hydrophobic tail, was prepared with this method [8]. To prepare **7**, the nonsymmetric monomer M_5 was first synthesized from hydroquinone in two steps. Next, condensation of M_5 with boron trifluoride etherate as the catalyst in CH_2ClCH_2Cl afforded the four constitutional isomers, among which **5** is the one having all five ester functional groups on the same side. At last, compound **7** was obtained by refluxing a solution of **5** and 1,2-ethanediamine in ethanol (Fig. 2b).

The statistical process follows a simple principle. Penta-functionalized pillar[5]arenes can be prepared through the Lewis acid-catalyzed cyclization of asymmetrically functionalized 1,4-dialkyoxybenzenes (M_1) with paraformaldehyde or 1,4-dialkoxy-2,5-bis-(ethoxymethyl)benzenes (M_2). As a result, two key intermediates (M_A/M_B) are formed *via* Friedel-Crafts alkylation/dealkylation. Subsequently, through the oligomerization processes involving M_A and M_B, two types of isomeric dimers D_{syn} and D_{anti} are obtained, which is determined by how the two 1,4-alkoxylated benzene rings and the methylene bridges are positioned relative to each other (Fig. 3a). Following this step, further reaction leads to the formation of a structurally stable pentamer. As impacted by the completely random binding direction of the monomers, four structural isomers will be formed following the statistical process, and the ratio of them reaches 5:5:5:1 (Fig. 3b). However, the C_5-symmetric RDP[5]s required only takes up one sixteenth of the product (about 6%). It is therefore suggested that though the method of statistical process is simple in raw materials and steps, the most significant problem is the low separation rate of C_5-symmetric isomers required, which also directly limits the study on the application of RDP[5]s.

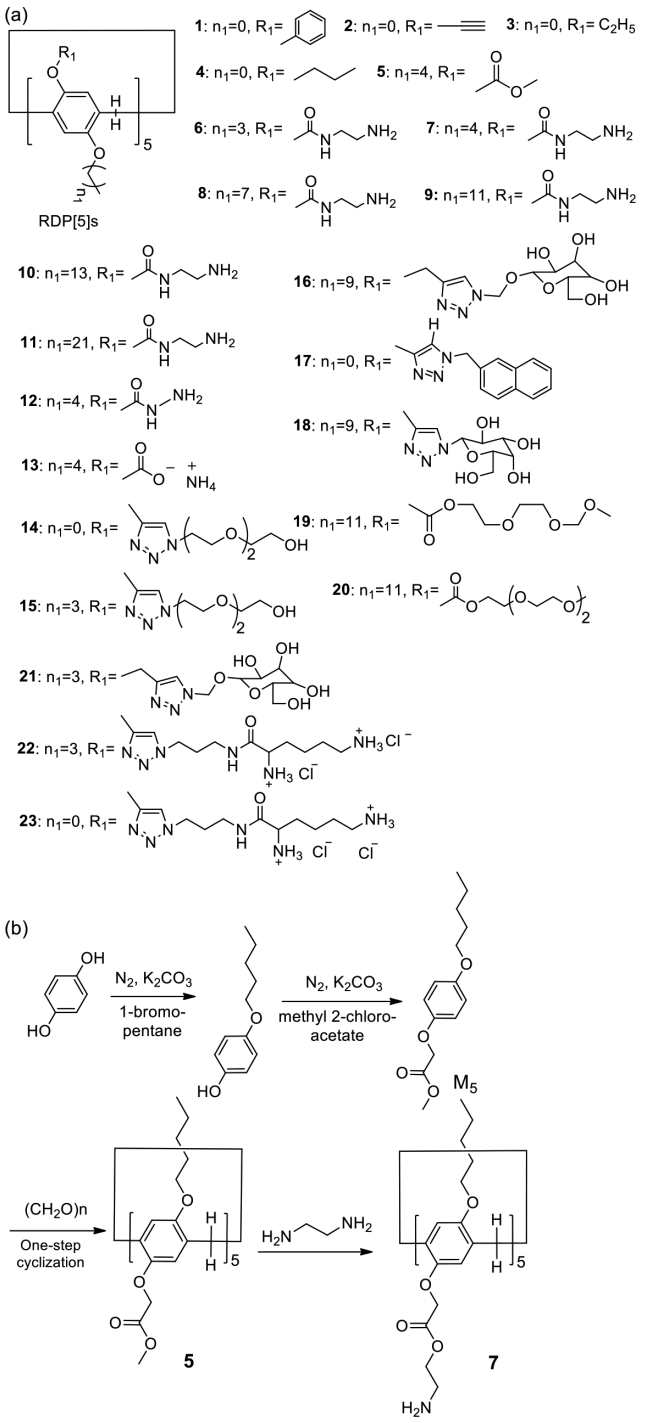

Fig. 2. (a) Partial rim-differentiated pillar[5]arenes synthesized by one-step cyclization. (b) Synthesis of amphiphilic RDp[5] **7**.

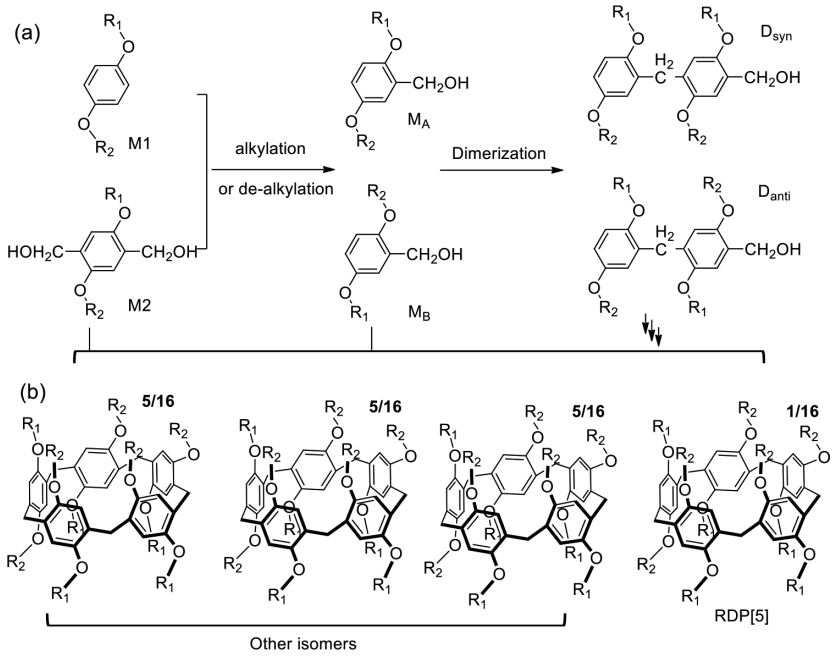

Fig. 3. (a) Lewis acid-catalyzed oligocyclization of 1,4-dialkyoxybenzenes (M_1) with paraformaldehyde or 1,4-dialkoxy-2,5-bis-(ethoxymethyl)benzenes (M_2). (b) The ratio of the isomers prepared from the one-step cyclization.

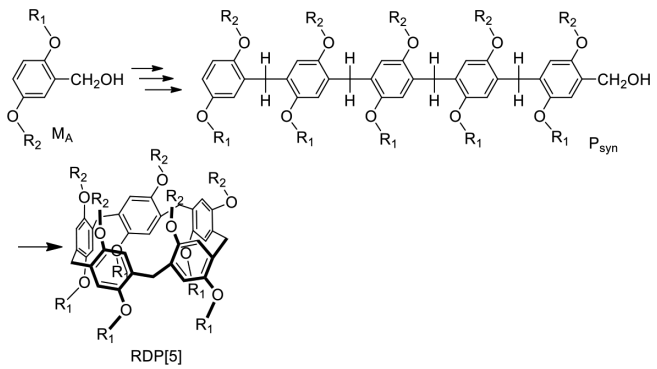

Fig. 4. The progress of the "pre-oriented" synthetic strategy.

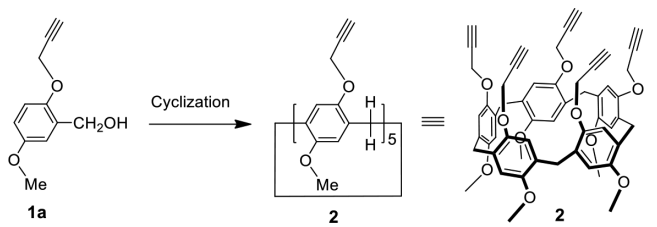

Fig. 5. The "pre-oriented" synthetic strategy for RDP[5] **2**.

2.2. "Pre-oriented" synthetic strategy

In 2018, Sue *et al.* proposed the "pre-oriented" synthetic strategy [9] to improve the existing situation that the synthetic yield of RDP[5]s is significantly low. The synthesis of the four isomers resulting from the statistical process is attributed to the formation of the two key intermediates (M_A/M_B), as well as the random combination of them. In this "pre-oriented" synthetic strategy, the structure of the intermediate is defined as the position of the methylene handle. For this reason, the direction will not be reversed during the polymerization, which improves the yield of RDP[5] (Fig. 4).

Sue *et al.* investigated the synthesis of RDP[5] **2** to verify the effectiveness of the method first. Following the statistical synthetic protocol, the mixture of $(propargyl)_5$-P[5] isomers was synthesized through the condensation reaction of 1-methoxy-4-(prop-2-yn-1-yloxy)-benzene with paraformaldehyde catalyzed by trifluoroacetic acid in 1,2-dichloroethane (DCE). Though the yield of the four isomers took up 78%, only 7% of them were required RDP[5]s. Subsequently, the research group used monomer **1a** for the condensation reaction under the popular $BF_3{\cdot}Et_2O$-catalyzed cyclization conditions for pillar[5]arenes (Fig. 5). All four constitutional isomers achieved the yield of 22%, in which the ratio of the RDP[5] isomer **2** took up 17%. Though the overall calculated yield of **2** was only 3.7%, the 17% selectivity showed an encouraging deviation from the statistical protocol. Next, these researchers investigated the effects of different catalysts, solvents and reaction time on the product yield. As indicated from the results, the selectivity increased to > 50% with $FeCl_3$ and $FeBr_3$ as the Lewis acid, whereas other metal salts (*e.g.*, FeF_3, $AuCl_3$, $InCl_3$, $Sc(OTf)_3$, $ZnCl_2$ and AgOTf) did not lead to any pillar[5]arenes formation under the identical reaction conditions. On the solvent side, chlorinated solvents (*e.g.*, chloroform, dichloromethane and 1,2-dichloroethane) all lead to the similar yield and selectivity. Specific to the reaction time, the reaction is commonly completed in 4 h. According to the study, the optimal solvent was 1,2-dichloroethane, and the optimal catalyst was $FeCl_3$.

Subsequently several different monomers containing either "clickable" moieties or good leaving groups were prepared to study the scope of this novel strategy. The mentioned monomers were catalyzed by $FeCl_3$ in 1,2-dichloroethane to produce corresponding RDP[5]s (Table 1). All these RDP[5]s can be further derivatized through considerable routine reactions (*e.g.*, copper-catalyzed azide-alkyne cycloaddition (CuACC), thiol-yne/thiol-ene click chemistry, alkene metathesis, as well as simple S_N2 reactions).

Table 1
Syntheses of various RDP[5]s.

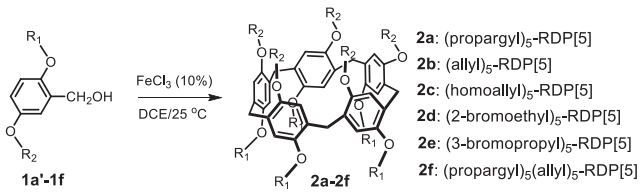

Entry	Substrate	R_1/R_2	Yield (%)	
			P[5]s	**2**
1	**1a'**	$CH_3/CH_2C{\equiv}CH$	34	19
2	**1b**	$CH_2CH{=}CH_2/Me$	32	16
3	**1c**	$CH_2CH_2CH{=}CH_2/Me$	38	18
4	**1d**	CH_2CH_2Br/Me	30	15
5	**1e**	$CH_2CH_2CH_2Br/Me$	19	9
6	**1f**	$CH_2CH{=}CH_2/CH_2C{\equiv}CH$	17	8

2.3. Functionalization at will strategy

Though the "pre-oriented" strategy significantly improves the yield of RDP[5]s, the synthesis of the respective type of RDP[5]s requires corresponding monomers with hydroxyethylene handle, and the synthesis of these monomers itself shows certain difficulties. In May 2019, Sue *et al.* proposed the functionalization at will of RDP[5]s by complying with the "pre-oriented" strategy [10]. Since hydroxyl groups are easily replaced by other groups, the optimization proposed a RDP[5] termed as $(OH)_5$-P[5] which have five hydroxyl groups on one rim and five methoxy groups on the other [11]. If 4-benzyloxyanisole is employed in the statistical process to synthesize $(OBn)_5$-P[5] and then hydrogenated to synthesize $(OH)_5$-P[5], the yield of the resulting $(OH)_5$-P[5] will be less than 1%, which certainly precludes any large-scale synthesis of multiple derivatives starting from this compound. Specific to the "pre-oriented" strategy, (2-(benzyloxy)-5-methoxyphenyl) methanol is reacted in 1,2-dichloroethane with $FeCl_3$ as the catalyst, and $(OBn)_5$-P[5] with the yield of 20% are obtained after straightforward column chromatography, followed by quick recrystallizaton. Subsequently, $(OBn)_5$-P[5] is hydrogenated, which quantitatively yields the corresponding penta-hydroxy$(OH)_5$-P[5]. Since the $(OH)_5$-P[5] are easy to re-oxidize in the air, further functionalization is required immediately after hydrogenation (Fig. 6).

According to existing studies, $(OH)_5$-P[5] was realkylated with propargyl bromide and NaH at 60 °C to afford pure $(propargyloxy)_5$-P[5] in 75% yield. Besides, $(OH)_5$-P[5] can be reacted with bromoacetonitrile to synthesize $(OCH_2CN)_5$-P[5], of which nitrile moiety can be reduced to the corresponding amine later on. Isotopic substitution is even possible *via* alkylation reactions, (*e.g.*, synthesis of $(OCD)_5$-P[5] with CD_3I and $(OH)_5$-P[5]).

Moreover, the mentioned route provides extra functional group tolerance for moieties that are incompatible with the Friedel-Crafts cyclization conditions to P[5], such as ester. The esterification by reacting $(OH)_5$-P[5] with acyl chlorides is capable of synthesizing numerous RDP[5]s that are hard to synthesize before, such as $(OCOMe)_5$-P[5] and $(OCOPr)_5$-P[5], with yields over 60%.

Besides alkylation and esterification, another alternative approach to functionalization of the –OH moieties of $(OH)_5$-P[5] refers to the sulfur(VI) fluoride exchange (SuFEx) reaction [12]. $(OH)_5$-P[5] received the clean reaction with sulfuryl fluoride gas in the presence of base to synthesize the corresponding fluorosulfate. This $(OSO_2F)_5$-P[5] could react with various aromatic *tert*-butyldimethylsilyl (TBS) ethers to give RDP[5]s with penta-OSO_2Ph, penta-OSO_2p-BiPh, as well as photoswitchable [13,14], OSO_2Ph-azobenzene moieties on one rim, respectively. All reactions proceeded in good to excellent isolated yields when the simple recrystallization or precipitation and MeOH washing were achieved. The SuFEx reactions show a significant potential to a broad range of RDP[5]s.

In existing routes, oxygen atoms directly attached to the column aromatic benzene ring were not removed. The functionality of RDP[5]s could be altered drastically if the O atom itself could be replaced, so, the electron density of the macrocyclic scaffold could be altered. For this end, and directly connected aryl groups on the P[5] core, $(OH)_5$-P[5] was converted to the corresponding pentatriflate, $(OTf)_5$-P[5], in 85% yield. This compound was engaged in Suzuki-Miyaura couplings to synthesize $(Ph)_5$-P[5] and $(p\text{-BiPh})_5$-P[5] in excellent isolated yields after straightforward column chromatography.

After the functionalizing one rim of the RDP[5]s, the final step refers to the modification of the other rim. On the whole, the alkoxy groups on both rims of RDP[5]s are difficult to remove selectively, thereby limiting the synthesis of novel RDP[5]s. However, robust C–C and OSO_2O linkages are generated *via* Suzuki-Miyaura couplings and SuFEx reactions, so the RDP[5]s could be further demethylated by the reaction with BBr_3 to form five hydroxyl groups on the other side. The mentioned compound can be further functionalized according to the above synthesis strategy. Lastly, the required RDP[5]s can be synthesized.

3. Self-assembly properties of rim-differentiated pillar[5]arenes

Due to the two different types of functional units on the rims of the RDP[5]s, they processed the interesting self-assembly properties. For instance, regioselective host-guest interactions can take place to an RDP[5] and a non-symmetric axle [17]. When one rim of RDP[5] is substituted with hydrophilic groups, and the other is substituted with hydrophobic groups, the RDP[5] can act as amphiphile. As a novel amphiphilic compound, amphiphilic RDP[5]s exhibit the rigid pillar-like structures to impart orientational organization, so they can form well-ordered structures from 0D micelles [15], 1D nanofibers, 2D membranes to 3D nanotubes [16] in aqueous solutions even at significantly low molecular weights. Moreover, the packing arrangements of these small anisotropic segments can rapidly transform into their equilibrium states when faced with very small environmental changes, which critically impacts the construction of responsive nanostructures [8].

3.1. Region-selective complexation

Since the functional groups on the two rims of perfunctionalized pillar[5]arene are identical, the directionality of the complexation should be controlled. For the different functional groups on the two rims of the RDP[5]s, their affinity with different groups are also different. Thus, they can conduct oriented host-guest complexation. In 2014, Li *et al.* synthesized a RDP[5] (**4**) containing five methyl groups on one rim and five *n*-pentyls on the other rim and investigated its complexation on 5-bromovaleronitrile [17]. First, as indicated from the complexation of **4**, per-methylated pillar[5]arene (DMP5A), and per-*n*-prentylated pillar[5]arene (DPP5A) towards monosubstituted butane guests, 1-bromobutane and 1-butyl cyanide, using ^{1}H NMR indicated that methyl side of pillar[5]arene is suitable for binging CN and the pentyl side is suitable for Br (Fig. 7). Compound **4** was subssequently complexed with the non-symmetric 5-bromovaleronitrile axle. Besides, as proved by NMR and X-ray analysis, **4** can regioselectivily engulf the 5-bromovaleronitrile axle to form an interpenetrated complex with a specific directionality of CN@methyl and Br@pentyl rim. The extension of this approach can achieve novel supramolecular assemblies with high-order topologies.

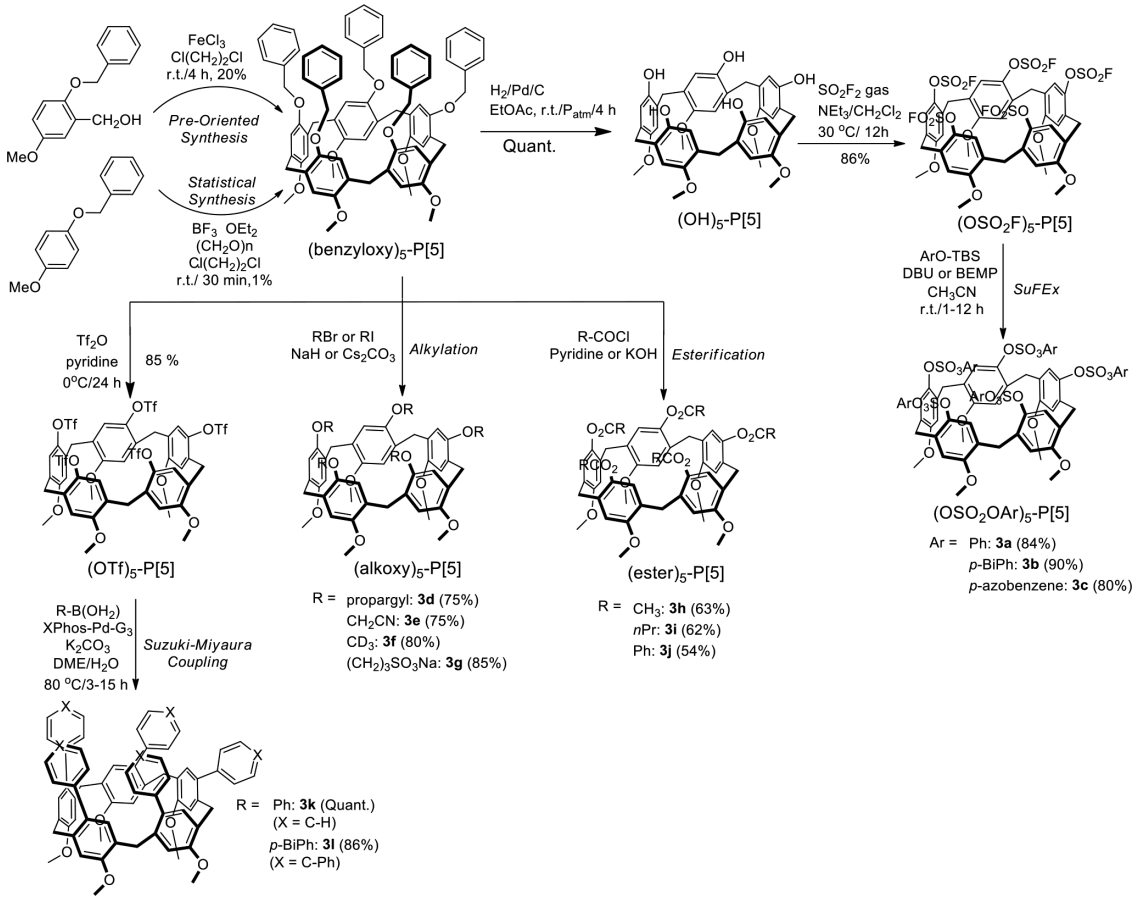

Fig. 6. A divergent synthetic route, starting from the gram-scale synthesis of a common penta-hydroxy rim differentiated pillar[5]arene precursor $(OH)_5$-P[5].

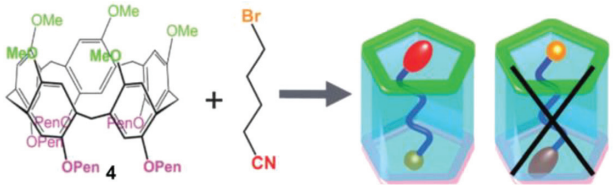

Fig. 7. Chemical structures of the RDP[5] **4** and the region-selective wheel/axle molecules. Reproduced with permission [17]. Copyright 2014, the Royal Society of Chemistry.

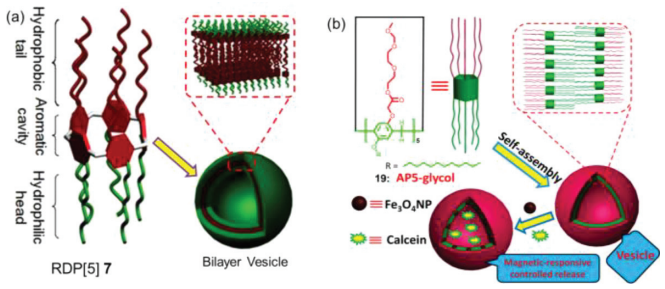

Fig. 8. (a) Cartoon illustration of RDP[5] **7** self-assembly into bilayer vesicles. Reproduced with permission [8]. Copyright 2012, American Chemical Society. (b) Chemical structure of RDP[5] **19** and it self-assembly into bilayer magnetic-responsive vesicle. Reproduced with permission [21]. Copyright 2014, American Chemical Society.

3.2. Vesicular structures

When RDP[5]s contain both hydrophilic and hydrophobic groups, and the ratio of hydrophilic/hydrophobic decreases to an appropriate value, the RDP[5]s tend to be self-assembled into vesicular structures. In 2012, as reported by Huang *et al.* found that the RDP[5] **7** could form vesicles in water. Through DLS, SEM and TEM, they confirmed that the diameter of the vesicle was nearly 200 nm, and the wall thickness was approximately 4 nm, about twice the length of the **7**, indicating that they are bilayer vesicle [8]. Xue *et al.* suggested that when the hydrophilic group was the same with **7**, whereas the hydrophobic units were other alkyl chains with different lengths, they could also form bilayer vesicles [19], demonstrating that the hydrophilic group critically impacts self-assembly (Fig. 8a). However, in 2014, Diao *et al.* prepared another RDP[5] **19** with five oligomeric glycol groups as the hydrophilic heads. DLS studies, TEM and SEM images were used to characterize the self-assembly process and the resulting assemblies, demonstrating that **19** could spontaneously form stable bilayer vesicles in water [21]. Moreover, oleic-acid-stabilized magnetic iron oxide nanoparticles could be incorporated into the bilayer of the vesicles to form hybrid magnetic-responsive supramolecular vesicles (Fig. 8b).

3.3. Micellar structures

When RDP[5]s contain five large hydrophilic groups on one rim and five small hydrophobic groups on another rim, they can exhibit amphiphilic properties and commonly be self-assembled into micellar structures when dispersed in water with a concentration over the critical aggregation concentration (CAC). For instance, in 2013 Sakurai *et al.* discovered a new RDP[5]s **22** with polar lysine head groups and found it spontaneously self-assembled into mi-

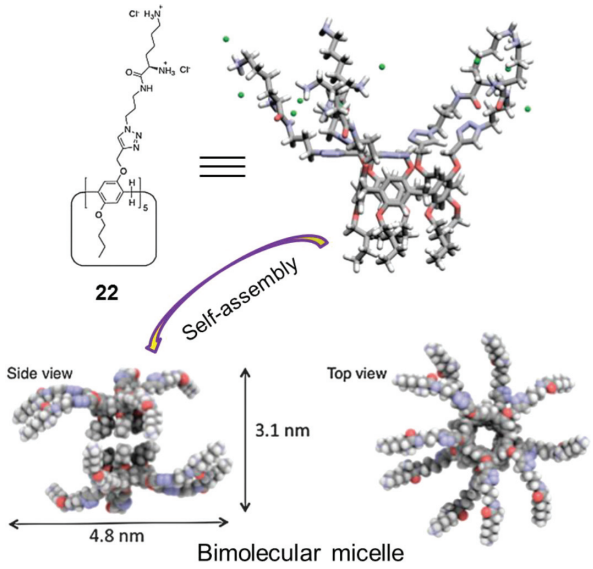

Fig. 9. The illustration of self-assembly of **22**-based bimolecular micelle. Reproduced with permission [18]. Copyright 2013, the Royal Society of Chemistry.

celles in water [18]. They characterized the self-assembled structure by using small angle X-ray scattering (SAXS), field flow fluctuation coupled with multi-angle light scattering (FFF-MALS) and atomic force microscopy (AFM). As indicated from the results, the **22** formed a stable bimolecular micelle in which the alkyl tails faced each other, and the hydrophobic portions were entirely covered by the long hydrophilic groups (Fig. 9).

Sometimes in the case of external stimuli, other self-assembly structures can also be converted into micelles. In 2012, Huang *et al.* synthesized a RDP[5] **7** containing five amino groups as the hydrophilic head and five alkyl chains as the hydrophobic tail [8]. As reported from the experiments under transmission electron microscopy (TEM), dynamic light scattering (DLS), and scanning electron microscopy (SEM), when it is dissolved in water, it can form vesicles, whereas when the pH of the solution decreases, the self-assembly structure can be micelles. The result can be explained by considering a pH-triggered vesicle-to-micelle transition. The decrease in pH results in the quarterisation of the amine groups. This increases the surface area of the hydrophilic headgroup, triggering the collapse of the vesicular structure into a micellar structure. In 2014, Xue *et al.* found that the RDP[5]s **6** and **7** could reversibly control the self-assembly structure of this RDP[5] from vesicles to micelles by bubbling CO_2 and N_2 [19].

3.4. Tubular structures

When there are extra intermolecular interactions (H-bonds or π–π stacking), the micelles or vesicles can be further self-assembled into tubular structures. Moreover, the assembled structures of the aggregates formed by the building blocks are determined by the curvature of the membrane. Typically, low membrane curvature tends to form a vesicular structure, while high membrane curvature tends to form a nanotubular structure. In 2012, Huang *et al.* found that there were some floccules in the solution of vesicles formed by **7** with five amino groups and five alkyl chains after staying 2 weeks. Over the culture time, the floccules gradually grew larger and darker. Based on SEM, TEM, AFM and UV–vis spectroscopy, the floccules were confirmed to be multilayer micro-tubes (Fig. 10) [8]. In 2013, they decorated **7** on the surfaces of gold nanoparticles and the **7**-stabilized gold nanoparticles can be self-assembled into the hybrid tubular structures. In addition, in 2013, they synthesized a sugar-functionalized RDP[5] **16**

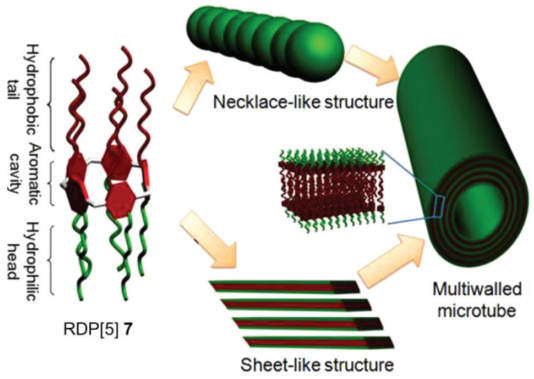

Fig. 10. Cartoon illustration of RDP[5] **7** self-assembly into multi-walled microtubes. Reproduced with permission [8]. Copyright 2012, American Chemical Society.

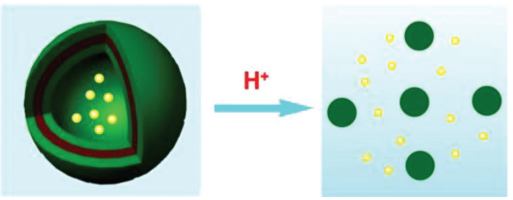

Fig. 11. Schematic representation of a pH-triggered vesicle-to-micelle transition of the aggregates of **7** and the subsequent release of encapsulated calcein. Reproduced with permission [8]. Copyright 2012, American Chemical Society.

that could rapidly self-assemble into vesicles in water through van der Waals interactions. After a week, as impacted the combined action of intermolecular hydrogen bonds and van der Waals interactions, the self-assembled structure further formed multi-layer microtubule structure [22], which was confirmed by applying SEM, TEM, UV–vis and FTIR spectroscopy.

4. Application of rim-differentiated pillar[5]arenes

According to the rapid development of RDP[5]s over the past few years, their special characteristic has been fully demonstrated. RDP[5]s exhibit a perfect symmetrical structure and more abundant properties than monomers. Moreover, they can become a novel amphiphilic compound when hydrophobic groups on the one rim and hydrophilic groups on the other, capable of being assembled into various spatial structures in aqueous solution. Over less than a decade, a number of researchers have reported numerous applications of RDP[5]s (*e.g.*, controllable releases [8], catalysis [20], bacterial cell agglutination, ion/molecular recognition, bioimaging and ion sensors).

4.1. Controlled release

When certain RDP[5]s are dispersed in water to be self-assembled into vesicles, they can encapsulate hydrophilic guest molecules inside the vesicles. If there is an external stimulant to induce the decrease in hydrophobic part or increase in hydrophilic tails, the vesicles formed by RDP[5]s will be transformed into micelles, so all the encapsulated molecules are released. For example, Huang *et al.* encapsulated the calcein in vesicles made up of RDP[5]s **7** and found no leakage of entrapped calcein over a period of 1 day. However, exposure of the calcein-loaded vesicles to a pH 4 environment resulted in rapid and complete release of the encapsulated calcein (Fig. 11) [8]. This is because the decrease in pH causes the quaternization of the amine groups, which expands the surface area of hydrophilic headgroup. As a result, the vesicular structure is caused to collapse into a micellar structure with con-

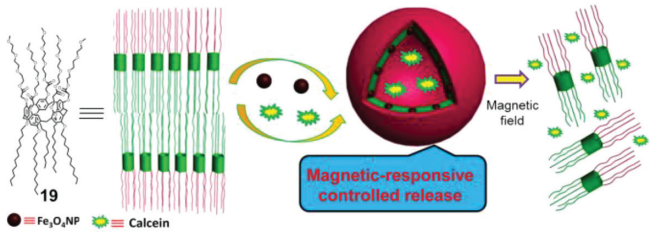

Fig. 12. Chemical structure of **19** and the schematic representation of the formation of bilayer vesicles, and further formation of magnetic hybrid vesicles in water. Reproduced with permission [21]. Copyright 2014, American Chemical Society.

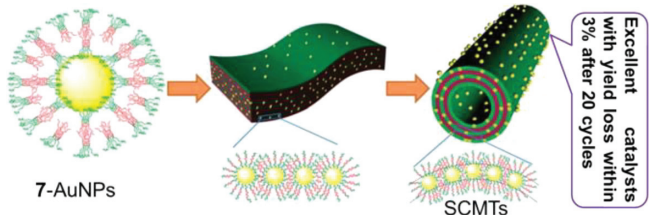

Fig. 13. Schematic representations of **7**-modified gold nanoparticles self-assembly into hybrid microtubes for green catalyst. Reproduced with permission [23]. Copyright 2013, the Royal Society of Chemistry.

comitant release of the encapsulated calcein. Later, as reported by Xue *et al.*, the self-assembly structures of this RDP[5]s and **6** can be reversibly controlled from vesicles to micelles by bubbling CO_2 and N_2 for their reversible reaction ability with CO_2 in water, providing a novel insight into the application of controllable releases [19].

Diao *et al.* prepared a new RDP[5] **19** with five oligomeric glycol groups and five alkyl chains, which can spontaneously self-assembly into bilayer vesicles, and incorporated oleic-acid-stabilized magnetic iron oxide nanoparticles into the bilayer of the vesicles to form hybrid magnetic-responsive supramolecular vesicle [21]. The calcein was encapsulated in the hybrid vesicles (Fig. 12). Fluorescence spectra showed that there was almost no leakage of entrapped calcein in one night without external magnetic field. However, exposing the system to an external magnetic field can result in the release of the encapsulated calcein.

4.2. Catalysis

Gold nanoparticles are capable of interacting with the microtube free-amide groups by hydrogen bonds. Thus, Huang *et al.* in 2013 stabilized gold nanoparticles by RDP[5] **7** and decorated them on the surfaces of microtubes prepared from the self-assembling of the RDP[5] **7** to form template composite microtubules (TCMTs) (Fig. 13). Moreover, gold nanoparticles can be used to fabricate self-assembled composite microtubes (SCMTs) without any external assistance, which has been confirmed based on UV–vis spectra, Fourier transform-infrared spectroscopy, TEM, SEM, X-ray diffraction measurements and thermogravimetric analysis [23]. It is noteworthy that the properties of the two composite microtubules are slightly different. Non-self-assembled gold nanoparticles might lose their activity during the reaction, which limits their reuse in nano-catalysts. However, SCMTS are stable at high temperatures, with strong acids, with strong bases, and under sonication, so they can act as an excellent catalyst. The research group showed that SCMTs could be used to reduce *p*-nitroaniline to 1,4-diaminobenzene with borohydride, and the yield loss was less than 3% for 20 cycles. This provides a new idea for the application of RDP[5]s in catalysis.

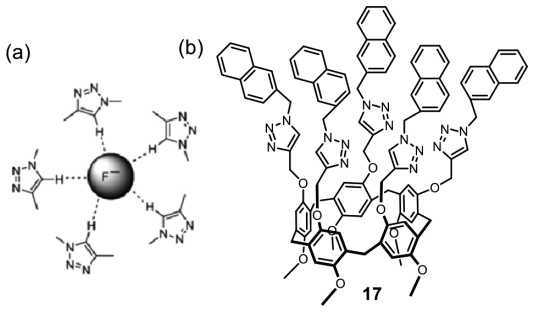

Fig. 14. (a) binding of the fluoride anion by multiple triazole groups of **17**; (b) chemical structure of **17**. Reproduced with permission [24]. Copyright 2012, the Royal Society of Chemistry.

4.3. Anion/molecular detection

In 2012, Huang *et al.* designed and synthesized a novel nonsymmetric pillar[5]arene-based anion receptor **17** with multiple triazole anion-binding sites (Fig. 14) [24]. The fluorescence titration experiments, ^{1}H NMR spectra, ^{19}F NMR spectra and NOESY NMR spectroscopy were employed to confirm that the RDP[5]s exhibit high selectivity and affinity for fluoride anion. It is noteworthy that the binding ability of the monomers that constitute the RDP[5]s with fluoride ions is significantly lower than that of the RDP[5]s with fluoride ions. This is attributed to the unique geometric of the RDP[5]s, which forms multiple C–H···F hydrogen-bonding interaction between the RDP[5]s and the fluorine anion, which noticeably improves their affinity. This novel pillar[5]arene-based neutral anion receptor enriches the structural diversity of anion binding chemistry, and it can be further adopted to fabricated sensing devices for the fluoride anion.

In 2013, Diao *et al.* modified the surface of reduced graphene oxide (ROG) with RDP[5]s **7** to form RGO-AP5 nanocomposite, which could be dispersed in water. Next, the amino groups on the RDP[5]s were connected with the gold nanoparticles (AuNPs) to form the RGO-AP5-AuNPs ternary nanocomposites [25]. During the host-guest electrochemical recognition, the nanocomposite could exert their respective advantages (*e.g.*, the excellent conductivity and large surface area of RGO, selective supramolecular recognition and enrichment capability of RDP[5]s, and the catalytic property of AuNPs), so the electrochemical response for the guests could be enhanced (Fig. 15). As indicated from the results, the RGO-AP5-AuNPs had excellent electrochemical analyzing performance on dopamine, with broad linear range and low detection limit at a signal-to-noise ratio of 3. This research provided a general idea for fabricating other ternary nanocomposites RGO-macrocyclic-metal nanoparticles that can synergistically enhance certain functions for many technological applications.

4.4. Biological application

In 2013, Huang *et al.* designed and synthesized a novel sugar-functionalized RDP[5] **16** containing galactose groups as the hydrophilic part and alkyl chains as the hydrophobic part (Fig. 16) [22]. As confirmed by TEM, SEM and fluorescence microscopy, it could self-assemble into nanotubes in water. The galactoses on the nanotubes provides multivalent ligands that exhibit high affinity for carbohydrate receptors on *E. coli*, and these nanotubes exhibit low toxicity to both cancer and normal cells, so they turn out to be excellent cell glues to agglutinate *E. coli.* Though the amphiphilic model compound which constitutes the **16** can self-assembly into vesicles, its ability to agglutinate *E. coli* decreased dramatically. As suggested from the mentioned results, supramolecular self-assemblies composed of simple ligands driven by noncovalent in-

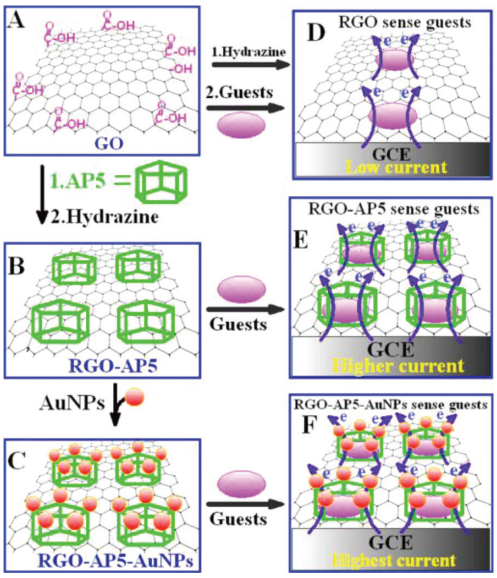

Fig. 15. Schematic diagram of (a) RGO, (b) RGO-AP5, and (c) RGO-AP5-AuNPs sensing the guest molecule by cyclic voltammetry. Reproduced with permission [25]. Copyright 2013, American Chemical Society.

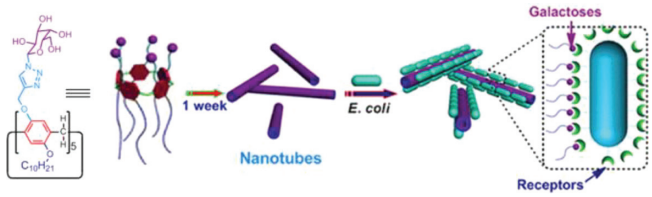

Fig. 16. Schematic representation of the self-assembly progress of **16**. Reproduced with permission [22]. Copyright 2013, American Chemical Society.

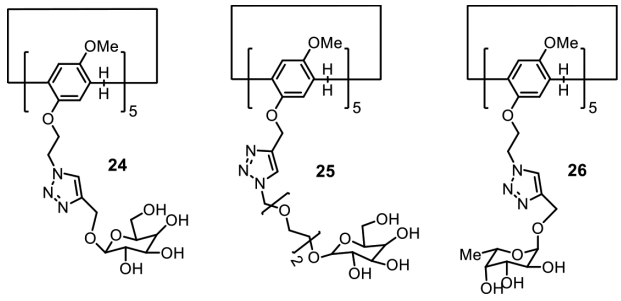

Fig. 17. Chemical structures of RDP[5]s **24, 25** and **26**.

teractions are chemical tools for capturing lining bacteria in solution.

Inspired by the mentioned studies, Vidal *et al.* synthesized several types of pentavalent pillar[5]arene-based glycoclusters and studied their multivalent binding to pathogenic bacterial lectins [26]. HIA, ELLA, ITC and SPR were employed to assess the binding properties of two glycoclusters **24** and **25** with LecA from *Pseudomonas aeruginosa*. As indicated from the result, the binding is heavily dependent of linker length between the core and carbohydrate, and this also impacts stoichiometry. Next, ITC was taken as the single technique to assess the dependence of binging of glycocluster **26** to LecB from *P. aeruginosa* and BambL from *B. ambifaria*. This glycociuster that was proved to be an excellent ligand for BambL with low nanomolar affinity whereas no improvement in binding compared with a monovalent ligand was observed for LecB, thereby demonstrating the importance of lectin topology in analyzing binding selectivity (Fig. 17).

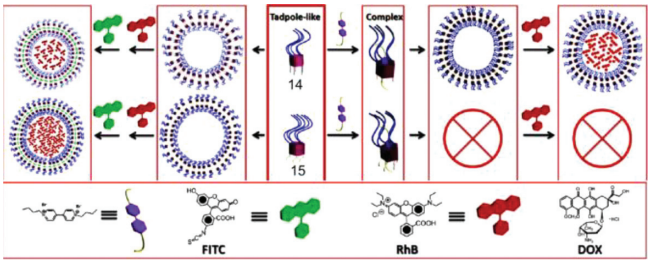

Fig. 18. Schematic representation of self-assemblies of RDP[5]s **14** and **15** as carriers for dual bio-imaging. Reproduced with permission [27]. Copyright 2013, American Chemical Society.

RDP[5]s was also applied in cell imaging. In 2013, Zhao *et al.* synthesized two tadpole-like RDP[5]s **14** and **15** by selectively employing water-soluble ethylene glycols and hydrophobic alkyl units as the starting materials. In comparison with their monomers, **14** and **15** show improved biocompatibility to cells and can form homogeneous supramolecular self-assemblies. Interestingly, different types of RDP[5]s-based assemblies achieve various performances on the delivery of dyes with different aqueous solubility. (**14, 15**)-based assemblies can deliver water-soluble rhodamine B to cells, as well as deliver hydrophobic fluorescein isothiocyanate for imaging. In addition, pillar[5]arene derivatives **14** could complex with a viologen guest, further forming stable assemblies for bioimaging. In the mentioned scenarios, the assembly formed from the complex of tadpole-like RDP[5] **14** with the viologen guest performed better in delivering mixed dyes (Fig. 18) [27].

5. Summary and outlook

In this Review, the synthesis, self-assembly properties and applications of rim-differentiated pillar[5]arenes (RDP[5]s) are described. The synthesis of RDP[5]s has been a difficult problem for a long time because of the C_5-symmetricl structure of these pillar[5]arenes, and the yield and separation rate are always very low. Over the past two years, researchers have continuously proposed optimized synthetic schemes, which significantly increased the yield of RDP[5]s and expanded the application range of RDP[5]s. More importantly, as impacted by their highly symmetrical structures, RDP[5]s have properties that are not present in the repeat unites, and their applications are relatively wider. When one rim of the RDP[5]s is hydrophobic, and the other is hydrophilic, the compound can act as a novel type of amphiphilies with a rigid columnar structure. Consistent with the formation of phospholipid bilayer, amphiphilic RDP[5]s can be self-assembled in solution into various well-defined nanostructures (*e.g.*, 0D micelles, 1D nanofibers, 2D membranes and 3D nanotubes). The RDP[5]s have been extensively employed in numerous areas (*e.g.*, green catalysis, controllable release, bacterial cell agglutination, ion/molecular recognition, bioimaging and ion sensors). Since the study of RDP[5]s remains preliminary, there is still considerable potential to be discovered, such as their application in adsorption.

So far, the RDP[5]s studied are pillar[5]arenes and pillar[6]arenes are almost absent. Due to the larger electron-donor cavities of pillar[6]arenes than pillar[5]arenes, their properties will be quite different. It is necessary to design and synthesize larger cavity pillar[5]arenes ($n \geq 6$) and study their applications. In addition, although the yield of the newly proposed functionalization at will of RDP[5]s based on the "preoriented" synthetic strategy is much higher than that of the original scheme, the synthesis steps are complicated, and the $(OH)_5$-P[5] are easy to be oxidized in the air. More importantly, the yield of this method for the synthesis of RDP[5]s is not high enough to be used on a large scale.

For this reason, RDP[5]s indeed show a promising future. RDP[5]s with different functional groups have C_5-symmetric structures and have been employed for controllable release, green catalysis, cell aggregation, ion/molecular detection, as well as bioimaging. In the future they may also be applied in biology, medicine and even water and air treatment.

Declaration of competing interest

The authors declare that they have no known competing financial interests or personal relationships that could have appeared to influence the work reported in this paper.

Acknowledgments

This work was supported by the National Natural Science Foundation of China (No. 21801139), Natural Science Foundation of Jiangsu Province (No. BK20180942), Six Talent Peak Projects in Jiangsu Province (No. xcl-085) and the scientific and technological activities for overseas students foundation of Shanxi Province (No. 20200025).

References

[1] (a) V.T. D'Souza, K.B. Lipkowitz, Chem. Rev. 98 (1998) 1741–1742;
(b) P.Y. Li, Y. Chen, C.H. Chen, Y. Liu, Chem. Commun. 55 (2019) 11790–11793;
(c) Y. Kobayashi, A. Harada, H. Yamaguchi, Chem. Commun. 56 (2020) 13619–13622.
[2] (a) W.A. Freeman, W.L. Mock, N.Y. Shih, J. Am. Chem. Soc. 103 (1981) 7367–7368;
(b) T. Jiang, G. Qu, J. Wang, et al., Chem. Sci. 11 (2020) 3531–3537;
(c) K. Kim, N. Selvapalam, Y.H. Ko, et al., Chem. Soc. Rev. 36 (2007) 267–279.
[3] (a) S.B. Nimse, T. Kim, Chem. Soc. Rev. 42 (2013) 366–386;
(b) M. Giuliani, I. Morbioli, F. Sansone, A. Casnati, Chem. Commun. 51 (2015) 14140–14159.
[4] (a) T. Ogoshi, S. Kanai, S. Fujinami, et al., J. Am. Chem. Soc. 130 (2008) 5022–5025;
(b) D. Cao, Y. Kou, J. Liang, et al., Angew. Chem. Int. Ed. 48 (2009) 9721–9723;
(c) S. Sun, M. Geng, L. Huang, et al., Chem. Commun. 54 (2018) 13006–13009;
(d) J. Wu, J. Tian, L. Rui, W. Zhang, Chem. Commun. 54 (2018) 7629–7632;
(e) X. Li, Z. Li, Y.W. Yang, Adv. Mater. 30 (2018) 1800177;
(f) H. Li, R. Wei, G.H. Yan, et al., ACS Appl. Mater. Interfaces 10 (2018) 4910–4920;
(g) B. Hua, W. Zhou, Z. Yang, et al., J. Am. Chem. Soc. 140 (2018) 15651–15654;
(h) T. Ogoshi, T. Furuta, Y. Hamada, et al., Mater. Chem. Front. 2 (2018) 597–602;
(i) Y. Wang, M. Jin, Z. Chen, et al., Chem. Commun. 56 (2020) 10642–10645;
(j) B. Li, L. Cui, C. Li, Angew. Chem. Int. Ed. 59 (2020) 22012–22016;
(k) G. Sun, W. Qian, J. Jiao, et al., J. Mater. Chem. A 8 (2020) 9590–9596;
(l) Y. Cai, Z. Zhang, Y. Ding, et al., Chin. Chem. Lett. 32 (2021) 1267–1279.
[5] (a) N.L. Strutt, H. Zhang, S.T. Schneebeli, J.F. Stodart, Acc. Chem. Res. 47 (2014) 2631–2642;
(b) L. Gao, B. Zheng, W. Chen, C.A. Schalley, Chem. Commun. 51 (2015) 14901–14904;
(c) X.Y. Hu, L. Gao, S. Mosel, et al., Small 14 (2018) 1803952;
(d) L. Gao, B. Zheng, Y. Yao, F. Huang, Soft Matter 9 (2013) 7314–7319;
(e) H. Liang, B. Hua, F. Xu, et al., J. Am. Chem. Soc. 142 (2020) 19772–19778;
(f) X.Y. Hu, X. Wu, S. Wang, et al., Polym. Chem. 4 (2013) 4292–4297;
(g) M. Ni, Y. Guan, L. Wu, et al., Tetrahedron Lett. 53 (2012) 6409–6413;
(h) R. Chen, H. Jiang, H. Gu, et al., Org. Lett. 17 (2015) 4160–4163;
(i) Y. Chang, J.Y. Chen, J. Yang, et al., ACS Appl. Mater. Interfaces 11 (2019) 38497–38502;
(j) N.L. Strutt, S.T. Schneebeli, J.F. Stoddart, Supramol. Chem. 25 (2013) 596–608;
(k) J. Ye, R. Zhang, W. Yang, et al., Chin. Chem. Lett. 31 (2020) 1550–1553;
(l) Y. Cao, Y. Chen, Z. Zhang, et al., Chin. Chem. Lett. 32 (2021) 349–352;
(m) S. Fu, G. An, H. Sun, et al., Chem. Commun. 53 (2017) 9024–9027.
[6] (a) Y. Yao, X. Wei, J. Chen, et al., Supramo. Chem. 30 (2018) 1–9;
(b) Z. Li, Y.W. Yang, Acc. Mater. Res. (2021), doi:10.1021/accountsmr.1c00042;
(c) X.Y. Lou, Y.W. Yang, Adv. Mater. 32 (2020) 2003263;
(d) Y.F. Li, Z. Li, Q. Lin, Y.W. Yang, Nanoscale 12 (2020) 2180–2200;
(e) N. Song, X.Y. Lou, L. Ma, H. Gao, Y.W. Yang, Theranostics 9 (2019) 3075–3093;
(f) Y. Yao, J. Chen, C. Wang, J. Nantong University (Natural Science Edition) 18 (2019) 8–15.
[7] Y. Kou, Z. Fu, H. Tao, et al., Eur. J. Org. Chem. (2010) 6464–6470.
[8] Y. Yao, M. Xue, J. Chen, et al., J. Am. Chem. Soc. 134 (2012) 15712–15715.
[9] M. Guo, X. Wang, C. Zhan, et al., J. Am. Chem. Soc. 140 (2018) 74–77.
[10] P. Demay-Drouhard, K. Du, K. Samanta, et al., Org. Lett. 21 (2019) 3976–3980.
[11] T.F. Al-Azemi, M. Vinodh, F.H. Alipour, A.A. Mohamod, J. Org. Chem. 82 (2017) 10945–10952.
[12] J. Dong, L. Krasnova, M.G. Finn, K.B. Sharpless, Angew. Chem. Int. Ed. 53 (2014) 9430–9448.
[13] T. Ogoshi, K. Kick, T.A. Yamagishi, J. Am. Chem. Soc. 134 (2012) 20146–20150.
[14] T. Ogoshi, S. Takashima, T.A. Yamagishi, J. Am. Chem. Soc. 140 (2018) 1544–1548.
[15] T. Xiao, L. Qi, W. Zhong, et al., Mater. Chem. Front. 3 (2019) 1973–1993.
[16] D. He, W. Zhang, H. Deng, et al., Chem. Commun. 52 (2016) 14145–14148.
[17] X. Shu, W. Chen, D. Hou, et al., Chem. Commun. 50 (2014) 4820–4823.
[18] T. Nishimura, Y. Sanada, T. Matsuo, et al., Chem. Commun. 49 (2013) 3052–3054.
[19] Y. Yao, P. Wei, S. Yue, et al., RSC Adv. 4 (2014) 6042–6047.
[20] D. Mullangi, S. Nandi, S. Shalini, et al., Sci. Rep. 5 (2015) 10876.
[21] J. Zhou, M. Chen, G. Diao, ACS Appl. Mater. Interfaces 6 (2014) 18538–18542.
[22] G. Yu, Y. Ma, C. Han, et al., J. Am. Chem. Soc. 135 (2013) 10310–10313.
[23] Y. Yao, M. Xue, Z. Zhang, et al., Chem. Sci. 4 (2013) 3667–3672.
[24] G. Yu, Z. Zhang, C. Han, et al., Chem. Commun. 48 (2012) 2958–2960.
[25] J. Zhou, M. Chen, J. Xie, G. Diao, ACS Appl. Mater. Interfaces 5 (2013) 11218–11224.
[26] N. Galanos, E. Gillon, A. Imberty, et al., Org. Biomol. Chem. 14 (2016) 3476–3481.
[27] H. Zhang, X. Ma, K.T. Nguyen, Y. Zhao, ACS Nano 7 (2013) 7853–7863.